

# Effect of Cu and Mg on the wear properties of spray formed Al-22Si alloy

Dayanand M Goudar<sup>1</sup>, K. Raju<sup>2</sup>, V. C. Srivastava<sup>3</sup>, G. B. Rudrakshi<sup>4</sup>

<sup>1</sup>Department of Mechanical Engg, Tontadarya College of Engineering, Gadag–582101, India

<sup>2</sup>Department of Mechanical Engg, St. Joseph Engineering College, Mangalore–575028, India

<sup>3</sup>Metal Extraction and Forming Division, National Met. Laboratory, Jamshedpur–831007, India

<sup>4</sup>Department of Mechanical Engg, Basaveshwar Engineering College, Bagalkot–587 101, India

Corresponding Author: Dayanand M Goudar, [dayanand\\_goudar@yahoo.co.in](mailto:dayanand_goudar@yahoo.co.in)

## Abstract

In the present study, the effect of Cu and Mg on the wear behavior of spray formed Al-22Si alloy has been investigated and the same has been compared with that of its counterpart as-cast alloy. Al-22Si and Al-22Si-4Cu-1.7Mg alloys prepared by spray deposition process were hot pressed to reduce the porosity. The microstructures were examined by optical and scanning electron microscopes. The microstructure of spray formed Al-22Si alloy is fine and homogeneous and primary silicon phase distributed in the aluminum matrix evenly are fine and faceted having a mean size of 12  $\mu\text{m}$ . The microstructure of spray formed Al-22Si-4Cu-1.7Mg alloy exhibited equiaxed grain morphology with fine and uniform distribution of both primary and eutectic Si with fine Q-Al-Si-Mg-Cu phase and  $\theta$ -Al<sub>2</sub>Cu precipitates dispersed evenly in  $\alpha$ -Al matrix. In contrast the microstructure of as-cast Al-22Si alloy consisted of coarse plates of primary Si of size 350  $\mu\text{m}$  and eutectic Si needles. The as-cast Al-22Si-4Cu-1.7Mg alloy consisted of coarse primary Si with Chinese script like  $\theta$ -Al<sub>2</sub>Cu precipitates and needles of Q-Al-Si-Mg-Cu phase in  $\alpha$ -Al matrix. The wear study of both as-cast and spray formed and hot pressed alloys under an applied load of 10 to 50 N and sliding velocity of 0.4 to 1.5  $\text{ms}^{-1}$  indicated two distinct regimes of mild and severe wear. In both the regimes, the spray-formed and hot pressed alloys consistently indicated a low wear rate compared to that of as-cast alloys. The high wear resistance of spray formed and hot pressed Al-22Si and Al-22Si-4Cu-1.7Mg alloys were explained in the light of their microstructural modifications induced during spray forming and subsequent hot pressing.

**Keywords:** Spray forming, Al-Si alloy, Hot pressing, Hardness, Wear

## 1.0 Introduction

The increasing and extensive requirements of the automotive and aerospace industries have encouraged the design of advanced materials with high strength to weight ratio, low coefficient of thermal expansion and high wear resistance [Lai06]. The hypereutectic Al-Si alloy feature an excellent low coefficient of thermal expansion, low density and high wear resistance characteristic which have engendered considerable interest for these alloys for automobile and aerospace applications [Dhe06]. However, conventional casting methods lead to blocky coarse primary Si particles in combination with interdendritic eutectic Si phase which limits the wear

properties of hypereutectic Al-Si alloys [Dwi04]. In order to improve the wear properties of as-cast hypereutectic Al-Si alloys, a modification in composition is necessarily made by adding alloying elements such as Cu, Mg, Fe etc [Sri06]. Addition of Cu and Mg to hypereutectic as-cast Al-Si alloys enables the formation of coarse intermetallic  $Mg_2Si$ ,  $Al_2Cu$  phases and other intermetallic compounds such as  $Al_2CuMg$  and Al-Si-Cu-Mg. These coarse phases do not contribute to strength and their degree of influence on wear behavior depends on their distribution and size relative to the Si particles [Moh12]. High wear resistance is imparted to the alloy when  $Mg_2Si$ ,  $Al_2Cu$  and Al-Mg-Si-Cu phases are present in the form of fine particulates. Spray deposition process has emerged as a promising route for manufacturing of alloys, composites and structural materials with the benefits associated with the rapid solidification such as fine grained microstructure, increased solid solubility and fine primary and secondary phases. In the spray forming process, liquid droplets are first atomized from a molten metal stream, quickly cooled by an inert gas, deposited on a substrate, and finally built up to form a low-porosity deposit with a required shape [Lav96]. The objective of the present study was to make use of the combined effects of rapid solidification and the advantages of hypereutectic Al-Si alloy with Cu and Mg alloying elements. In this study, Al-22Si and Al-22Si-4Cu-1.7Mg alloys were spray formed and hot pressed. The microstructural features of both as-spray formed and hot pressed alloys were reported. The effect of the modified microstructure of spray formed alloys on the wear behavior were studied and compared with that of the as-cast alloys.

## 2.0 Experimental details

The chemical composition of Al-22Si and Al-22Si-4Cu-1.7Mg alloys is shown in Table 1. The details of spray forming set up employed in the present study have been described elsewhere [Day13]. In brief, spray forming process employed an annular convergent-divergent nozzle to create a spray of the melt. In each run 2.5 kg of alloy has been melted to a superheat temperature of 150°C in a resistance heating furnace. The molten metal is atomized by a free fall atomizer using  $N_2$  gas. The resultant spray is deposited over a Cu substrate resulting in a near net shaped preform. The process variables employed for producing the preforms are listed in Table 2.

**Table 1:** Chemical composition of Al-22Si and Al-22Si-4Cu-1.7Mg alloys

Alloy	Si	Cu	Fe	Ni	Mg	Al
Al-22Si	22	0.06	0.05	0.035	0.123	Bal
Al-22Si-4Cu-1.7 Mg	22	4.0	0.004	0.025	1.72	Bal

**Table 2:** Process variables in spray forming process

Melt super heat temperature	100°C
Atomizing gas	$N_2$
Gas pressure	0.45 MPa
Type of nozzle	Free fall
Nozzle to substrate distance	390 mm
Melt flow rate	2.48 kg/min
Diameter of the delivery nozzle	4 mm

Specimens of size 100 x 30 x 20 mm were cut from the preforms. The specimens were hot pressed at a pressure of 55 MPa and a temperature of 480°C for densification. The density of

spray formed alloys was measured by using Archimedes principle as per ASTM: B962 – 08. The percentage of porosity (% P) in the spray formed alloys was measured by using the actual density ( $\rho_{ac}$ ) and the theoretical density ( $\rho_{th}$ ) of the alloys using the relation, % P =  $[1 - (\rho_{ac} / \rho_{th})] \times 100$ . The samples were prepared by polishing using standard metallographic techniques of grinding on emery paper with 1/0, 2/0, 3/0 and 4/0 specifications and cloth polishing. The polished samples were etched with Keller's reagent (1% vol. HF, 1.5% vol. HCl, 2.5% vol. HNO<sub>3</sub> and rest water). The microstructures of the samples were examined under a ZEISS Optical Microscope and Scanning Electron Microscopy (S-3400N Hitachi Model). The hardness measurement was carried out using Vickers Hardness Tester (Mattoon ATK-600) at an applied load of 300g. Wear tests were conducted on all the alloy specimens on a pin-on-disc wear testing machine (Model: TR-20, DUCOM) as per ASTM: G99-05. The counterpart disc was made of quenched and tempered EN-32 steel having a surface hardness of 65HRC. Wear specimens of size  $\text{Ø}8 \times 30$  mm were machined out from both the alloys. The specimens were polished and then cleaned with acetone before conducting the wear test. The wear tests were conducted by varying load from 10–50 N at a sliding velocity of  $1.5 \text{ ms}^{-1}$  and a sliding distance of 1025 m. Similarly the sliding velocity of the disc was varied from 0.4 to  $1.4 \text{ ms}^{-1}$  at a constant applied load of 50 N. All the experiments were carried out under dry sliding conditions and data was recorded at room temperature. The worn surfaces of both the alloys after wear testing were examined under Scanning Electron Microscopy.

### 3.0 Results and discussion

#### 3.1 Microstructural features

Fig. 1 (a) shows the optical micrograph of as-cast Al–22Si alloy. It consists of large sized polyhedral shaped primary Si and needles of eutectic Si in the Al-matrix. The size of primary Si size ranges from 50 to 350  $\mu\text{m}$  and length of the eutectic silicon needles ranges from 20 to 50  $\mu\text{m}$ . Fig. 1 (b) shows the optical microstructure of as-cast Al–22Si–4Cu–1.7Mg alloy. The microstructure consists of coarse block like primary Si with eutectic network of Al-Si phase together with the intermetallic phases. SEM/EDS micrograph of as-cast Al–22Si alloy is shown in Fig. 2 (a). It consists of coarse primary Si particles in the form of plate like / fishbone structure while, eutectic phase comprises of Si needles randomly distributed in the Al-matrix. The phase composition of as-cast Al–22Si alloy is shown in Table 3.

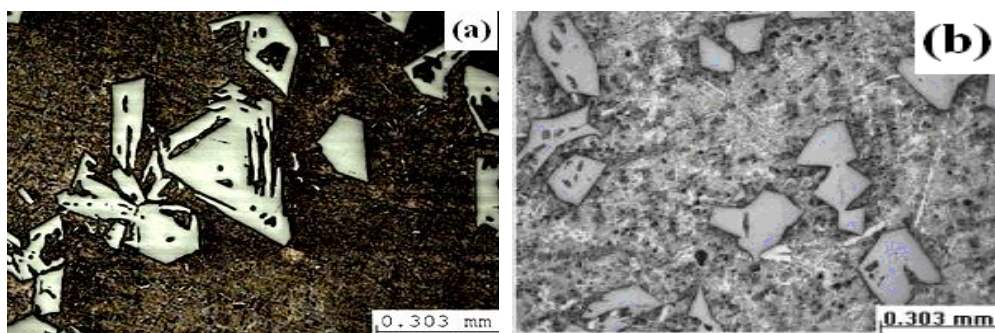


**Fig. 1:** Optical micrographs of as-cast (AC) alloys (a) Al–22Si (b) Al–22Si–4Cu–1.7Mg

SEM/EDS micrograph of as-cast Al–22Si–4Cu–1.7Mg alloy is shown in Fig. 2 (b) It is mainly composed of primary Si particles having sharp edged polygonal plate like morphology, Q phase, and  $\theta$ -Al<sub>2</sub>Cu phase exists in the form of needles /Chinese script distributed randomly in

the Al-matrix. The size of Si varies from 75–150  $\mu\text{m}$ . The EDS results of various phases present in the as-cast alloy is shown in Table 4.

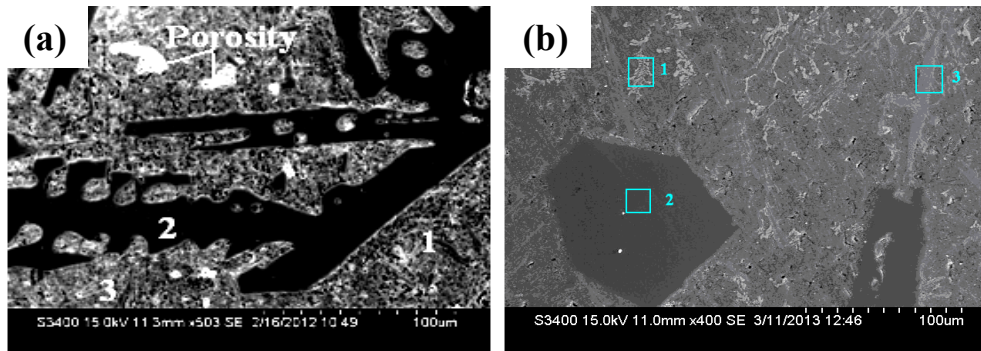


**Fig. 2:** SEM/EDS micrographs of as-cast alloys (a) Al-22Si (b) Al-22Si-4Cu-1.7Mg

**Table 3:** EDS analysis of as-cast Al-22Si alloy

Location	Composition	Phase	Al-K	Mg-K	Si-K	Fe-K
Point 1	$\text{Al}_{83}\text{Si}_{15}$	Eutectic phase	80.56	0.00	19.81	0.37
Point 2	$\text{Si}_{98}$	Si	0.14	0.05	99.72	0.00
Point 3	$\text{Al}_{99}$	$\alpha$ -Al Matrix	96.92	0.00	17.04	0.00

**Table 4 :** EDS analysis of as-cast Al-22Si-4Cu-1.7Mg alloy

Location	Composition	Phase	Al-K	Mg-K	Si-K	Cu-K
Point 1	$\text{Al}_2\text{Cu}_{15}$	$\text{Al}_2\text{Cu}$	45.73	1.14	0.00	50.16
Point 2	$\text{Si}_{98}$	Si	0.94	0.00	98.37	0.49
Point 3	$\text{Al}_{79}\text{Mg}_4\text{Si}_3\text{Cu}_1$	Q-phase	78.27	2.70	15.48	3.44

Fig. 3 (a) represents the optical micrograph of spray deposited Al-22Si alloy. The alloy consists of fine primary Si with spherical morphology having average size less than 10  $\mu\text{m}$ , the eutectic Al-Si phase has been finely divided into smaller particles and distributed uniformly throughout the Al matrix. A porosity of 11.6% with spherical morphology of micron size was observed in the spray deposited alloy. Fig. 3 (b) shows the optical microstructure of spray formed Al-22Si-4Cu-1.7Mg alloy. The microstructure consists of an equiaxed, nearly spheroidized grain morphology of  $\alpha$ -Al matrix. The Si particles are highly refined having a size varying from 2–25 $\mu\text{m}$ , Cu and Mg containing intermetallics are uniformly distributed in the Al-matrix. The presence of fine, spherical porosity of 15.2 % has been observed in the spray formed alloy. Fig. 4 (a) shows the SEM/EDS micrograph of spray deposited Al-22Si alloy. It can be seen from the micrograph that the alloy exhibited the primary Si particulates and fine eutectic Si phase which are uniformly distributed in Al-matrix. The EDS results of various phases present in the spray deposited alloy is shown in Table 5. The SEM/EDS micrograph of spray deposited Al-22Si-4Cu-1.7Mg alloy is shown in the Fig. 4 (b). The microstructure of alloy exhibited coexisting faceted primary Si particles and fine plates of complex intermetallic phases. The size of Si particles varied from 3 to 20  $\mu\text{m}$  compared to large particle size of 150  $\mu\text{m}$  in as-cast alloy. The various phases present are grey colored Si particulates as a major element, grey colored intermetallic Q- $\text{Al}_{48}\text{Si}_{29}\text{Mg}_{18}\text{Fe}_4$  phase and bright white phase of  $\theta$ - $\text{Al}_2\text{Cu}$ . The EDS results of various phases present in the spray deposited alloy is shown in Table 6.

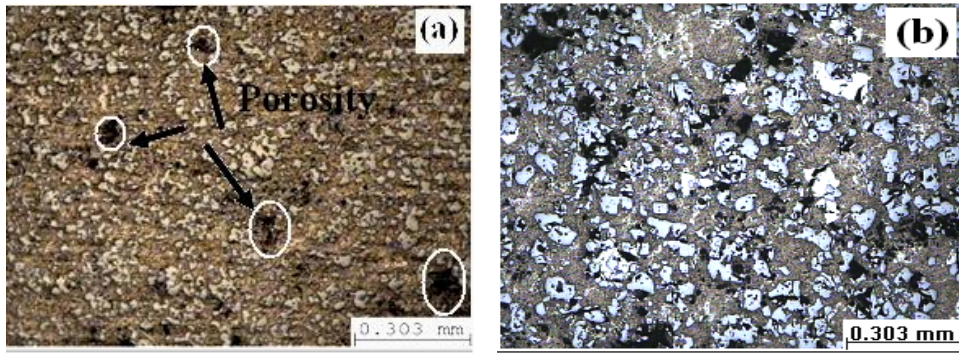


**Fig. 3:** Optical micrographs of spray deposited alloys (a) Al-22Si (b) Al-22Si-4Cu-1.7Mg

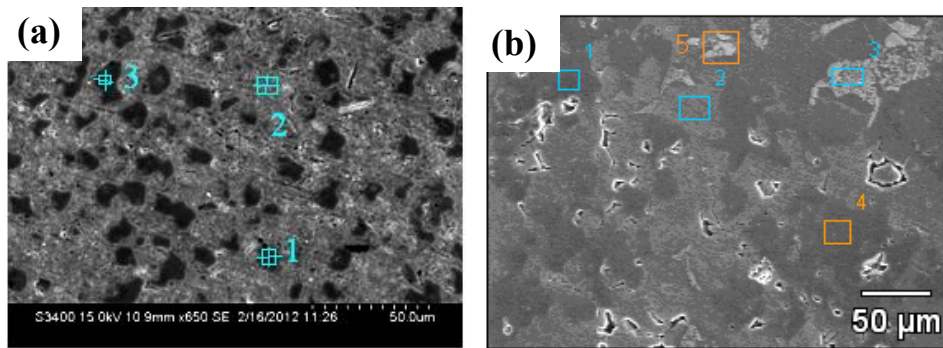


**Fig. 4:** SEM/EDS micrograph of spray deposited alloys (a) Al-22Si (b) Al-22Si-4Cu-1.7Mg

**Table 5:** EDS analysis of spray deposited Al-22Si alloy

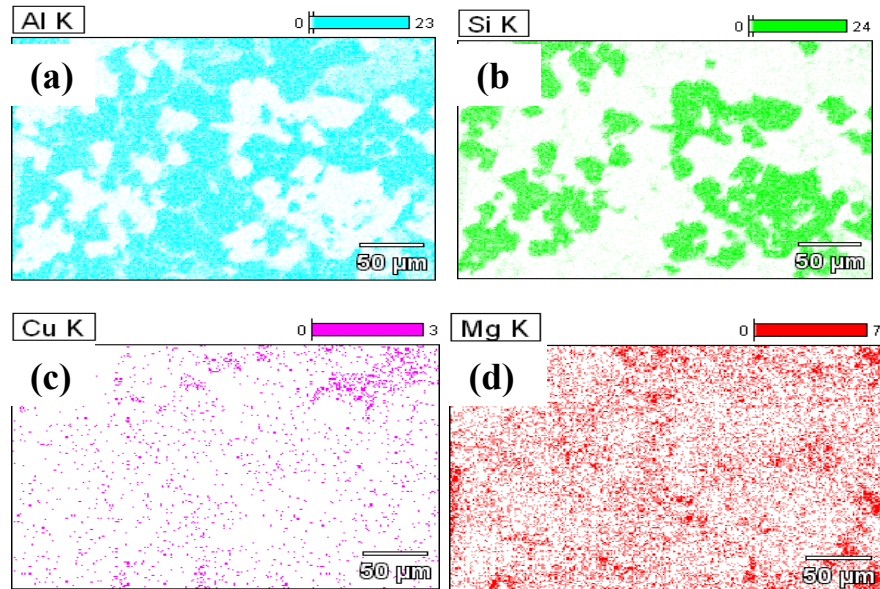
Location	Composition	Phase	Al-K	Mg-K	Si-K	Fe-K
Point 1	Al <sub>10</sub> Si <sub>88</sub>	Eutectic Si	11.22	0.05	88.30	0.00
Point 2	Al <sub>99</sub> Si <sub>1</sub>	α-Al Matrix	96.59	0.00	0.75	0.25
Point 3	Si <sub>98</sub> Al <sub>2</sub>	Si	1.62	0.12	98.11	0.00

**Table 6:** EDS analysis of spray deposited Al-22Si-4Cu-1.7Mg alloy

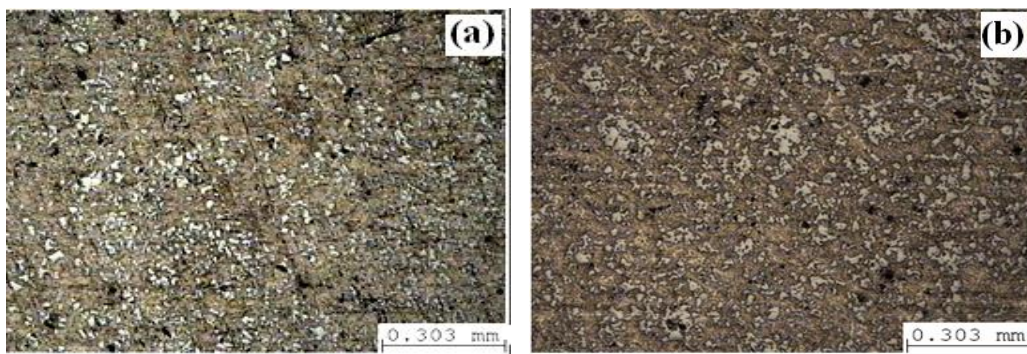
Location	Composition	Phase	Al-K	Mg-K	Si-K	Cu-K
Point 1	Si	Si	1.05	0.07	97.74	0.75
Point 2	Al matrix	Si	94.48	0.97	0.00	1.28
Point 3	Al <sub>2</sub> Cu	θ	56.09	2.11	1.17	37.88
Point 4	Si	Si	0.99	0.00	97.05	0.00
Point 5	Q – phase					

Fig. 5 shows the X-ray images of spray formed Al-22Si-4Cu-1.7Mg alloy. This reveals the presence of Si, Cu and Mg elements which are uniformly distributed in the spray formed alloy and is well corroborated with EDS results.

The optical microstructure of spray formed and hot pressed Al-22Si alloy is shown in Fig. 6 (a). This exhibits the fragmentation of primary Si particles, eutectic Si phase, significantly reduced porosity level of 5.4 % and increased volume fraction of Si phase. Fig. 6 (b) shows the optical micrograph of spray formed and hot pressed Al-22Si-4Cu-1.7Mg alloy. It can be observed from the Fig. 6 (b) that there is a fragmentation of Si and brittle θ and Q intermetallics and porosity has been reduced to 3.8 %.



**Fig. 5:** EPMA micrograph of spray formed Al-22Si-4Cu-1.7Mg alloy (a) Al (b) Si (c) Cu (d) Mg



**Fig. 6.** Micrographs of spray formed and hot pressed alloys (a) Al-22Si (b) Al-22Si-4Cu-1.7Mg

The solidification of as-cast Al-22Si and Al-22Si-4Cu-1.7Mg alloys, due to slow cooling rate and broad temperature interval between the liquidus and solidus of higher Si content composite in the pseudo binary section will cause castings with a coarse plate like Si, needle like Q and Chinese script like  $Al_2Cu$  phases. In spray forming process, the solidification phenomena changes due to the effect of high cooling rate during the atomization stage and the unique microstructural evolution mechanism after deposition. The fine uniform distribution of primary Si particles and eutectic Si phase and equiaxed morphology of the  $\alpha$ -Al phase are remarkable features of spray deposited hypereutectic Al-Si alloy. These features are due to the relatively high cooling rate ( $10^3$ - $10^6$  Ks<sup>-1</sup>) associated with repeated deformation and extensive fragmentation of partially solidified droplets during the build-up of the deposit which could effectively alter the morphological stability of the Si phase [Sri01]. As the cooling rate increases during atomization, the droplets experience a large undercooling prior to nucleation of primary Si phase leading to refinement. Simultaneously, reduced temperature suppresses the growth of these phases even after the deposition [Gra95]. Thus, large amount of fine and uniformly distributed Si and greater number of precipitates ( $Al_2Cu$  phase, Q phase) are seen in the spray formed Al-22Si-4Cu-1.7Mg alloy. The dendritic as well as the Chinese script structures observed

in the as-cast alloys are modified and it is difficult to discern the difference between primary Al<sub>2</sub>Cu and Q phases. The porosity has been observed in the deposits and was uniformly distributed. The spherical morphology and non-connected distribution of the pores suggest that their formation occurred due to the incorporation of gas, a well-described phenomenon caused by an excessive presence of liquid during the spray formation [Cai98]. Hot pressing of spray formed alloys led to a considerable reduction in porosity and recrystallization of microstructure to a certain extent. The preheating treatment before compression process can make the microstructure more uniform. Secondly, hot deformation leads to a microstructural refinement and a solid-state phase transformation. The severe stress imposed by hot compression generates high density dislocations in the grains. Subsequently, the movement and arrangement of dislocations form lot of small angle grain-boundaries, refining initial grains into several substructures. In addition to the refinement of grains, hot deformation also promotes homogeneous precipitation of hardening of  $\theta$  and Q phases which can pin the movement of dislocations to restrain grains coarsening during recrystallization effectively [Est90].

### 3.2 Hardness

The results of hardness measurement of spray formed + hot pressed (SF + HP) Al-22Si and Al-22Si-4Cu-1.7Mg alloys are as shown in the Table 7. It is observed from the results that a significant increase in the microhardness of SF+HP alloys takes place compared to as-cast alloys. The SF+HP Al-22Si-4Cu-1.7Mg alloy exhibits higher hardness compared to Al-22Si alloy. The increase in the hardness of spray formed + hot pressed Al-22Si alloy is due to the presence of fine and uniform distribution of Si particles in Al-matrix as well as reduction of porosity. It may be noted that an increase in the volume fraction of the Si particles will lead to higher constraint in the localized deformation of softer matrix under the application of indentation load. The fine primary Si and eutectic Si phases provide an appreciable impediment to plastic deformation caused by the indentation. The higher hardness of spray formed + hot pressed Al-22Si-4Cu-1.7Mg alloy can be attributed to the presence of fine and uniform distribution of brittle intermetallic  $\theta$ -Al<sub>2</sub>Cu and Q phases in addition to fine primary Si particles [Sha07, Hau09].

**Table 7:** Hardness of as-cast and SF + HP alloys

Alloy	Processing route	Hardness (VHN )
Al-22Si	As-cast	53
Al-22Si	SF + HP	83
Al-22Si-4Cu-1.7Mg	As-cast	67
Al-22Si-4Cu-1.7Mg	SF + HP	116

### 3.3 Wear characteristics

Variation in the wear rate of both the AC and SF + HP alloys as a function of applied load at constant sliding velocity of 1.5ms<sup>-1</sup> is shown in Fig.7. Wear rate of both as-cast and SF + HP alloys increases with increasing normal load. Comparative study of wear behavior of two alloys shows that SF + HP alloys are subjected to lower wear rate than as-cast alloys under identical sliding conditions. In the entire range of applied load, the SF + HP Al-22Si-4Cu-1.7Mg alloy exhibited best wear resistance.

Fig. 8 shows the effect of sliding velocity on the wear rate of the alloys. It is worthwhile to note that the wear rate initially decreases with increasing sliding velocity. With further increase in the sliding velocity beyond the critical limit, the wear rate increases irrespective of

alloy condition and composition. It is observed from the variation of wear rate with sliding velocity that the spray formed alloys show less wear rate than as-cast alloys. Minimum wear rate is observed in SF + HP Al-22Si-4Cu-1.7Mg alloy. Fig. 9 depicts the variation of coefficient of friction of Al-22Si and Al-22Si-4Cu-1.7Mg alloys. It can be seen that initially, the coefficient of friction decreased with increasing load and found to be constant in all the alloys with further increase in load. The spray formed and hot pressed alloys indicate lowest coefficient of friction, whereas the highest friction coefficients occurred in the as-cast alloys. The different wear characteristics of spray formed alloys are related to their microstructural features. The wear behavior of hypereutectic Al-Si alloys has been reported in several recent investigations [Dhe06, Cla79, Pra87, Sas92, Raj12].

In general, the size and shape of Si particles and the nature of dispersion of second phase particles in the matrix have been observed to have a strong influence on the wear rate of a wide range of materials. In the present work, the spray-formed and hot pressed alloys exhibit a uniform distribution of fine Si particles and distribution of hard intermetallics (Q-phase) and  $\theta$ -Al<sub>2</sub>Cu precipitates have a large influence on the dry sliding wear behavior of alloys [Haq01]. These features of the spray formed alloy are attributed to strong bonds at the matrix-particle interface due to the decrease in the particle size and the consequent microstructural stability of the alloy under a range of applied loads and sliding velocities. The block like Si particles, long needles of intermetallic Q-phase and coarse  $\theta$ -Al<sub>2</sub>Cu phase appear to have played an important role in aggravating the wear process in as-cast alloy. The sharp edges of Si particles and intermetallic Q-phase may have acted as crack nucleation sites resulting in a stress concentration that is more severe at the interface between the tip of needle-like intermetallic Q-phase and the Al-matrix that led to the fracture of long needles of Q-phase resulting in a high wear rate in as-cast alloy. The reduction in porosity, recrystallization and fragmentation of Q-phase and Al<sub>2</sub>Cu phase, their uniform distribution in the matrix of spray formed and hot pressed alloy, decrease the stress concentration between the fine needles of Q-phase and the matrix and increase the strength of matrix due to fine dispersion of Al<sub>2</sub>Cu, resulting in an improved wear resistance.

At low loads, more time is available for the formation and growth of micro-welds, which increases the force needed to shear-off the micro-welds to keep the relative motion and this leads to an increase in wear resistance. An increase in the load results in the rise of the interface temperature that engenders oxidation and thermal softening of material. The brittle and discrete oxide film is harmful because it acts as a hard impurity or third body between mating surfaces [Ana09]. The wear rate with normal load shows a linear relation up to the load of 40 N. Further increase in the load to 50 N shows an abrupt increase in wear rate indicating a change in the wear mechanism. At high loads, the thermal softening of the alloy in the sub surface region takes place leading to a large scale plastic deformation [Moh96]. Under such conditions, metallic wear takes place. The remarkable observation in the present study is that the fine distribution of Si, intermetallic phases and good interfacial bonding at the interface with the matrix provided by the fine precipitates of  $\theta$ -Al<sub>2</sub>Cu, allows for high temperature stability leading to a low wear rate in SF + HP Al-22Si-4Cu-1.7Mg alloy compared to SF + HP Al-22Si alloy. The dispersoids of intermetallics phase in Al-22Si-4Cu-1.7Mg alloy possess higher hardness compared to that of eutectic Si phase in Al-22Si alloy. The low melting constituent of eutectic Si is smeared out on mating surfaces at an early stage. This effect arises due to small interparticle spacings of dispersoids in spray-formed Al-22Si-4Cu-1.7Mg alloy.

Consequently, a thin oxide layer is developed on the surface of wear test specimen which protects the materials from further wear. The low wear rate of SF + HP Al-22Si-4Cu-1.7Mg



alloy justifies this mechanism. However, the stability of the oxide layer on the specimen surface depends on applied load and sliding velocity of the mating surfaces. The experimental result indicates that the stability regime of the oxidation film is extended to higher load and sliding velocity in the mild wear regime of the SF + HP alloys. However, as the sliding velocity is further increased, instability arises in the continuity of the oxidation layer. This is indicated by a significantly high wear rate of the material with further increase in the sliding velocity. Still in this severe wear regime, the SF + HP alloys, owing to the uniformly distributed Si and small inter particle spacing of its fine Si particles and intermetallics, continues to provide a relatively low wear rate compared to the as-cast alloys.

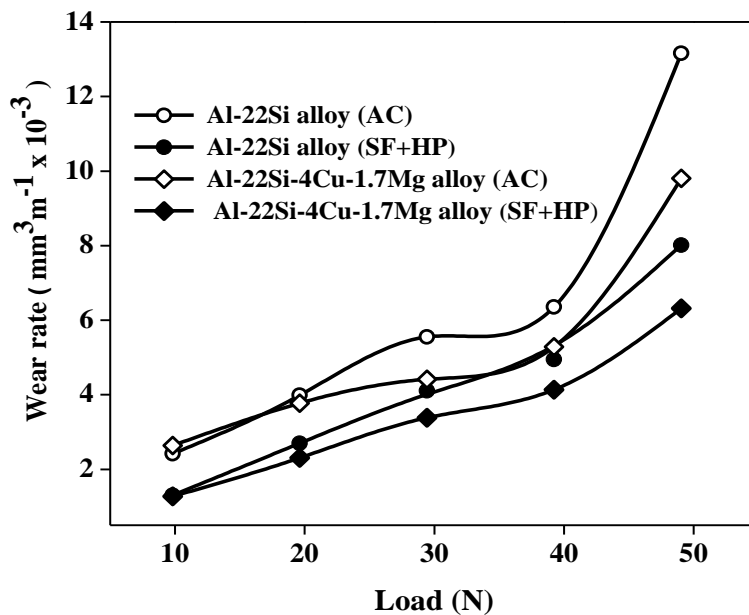


Fig. 7: Variation in wear rate with load of AC & SF + HP alloys at a sliding velocity of  $1.5 \text{ ms}^{-1}$

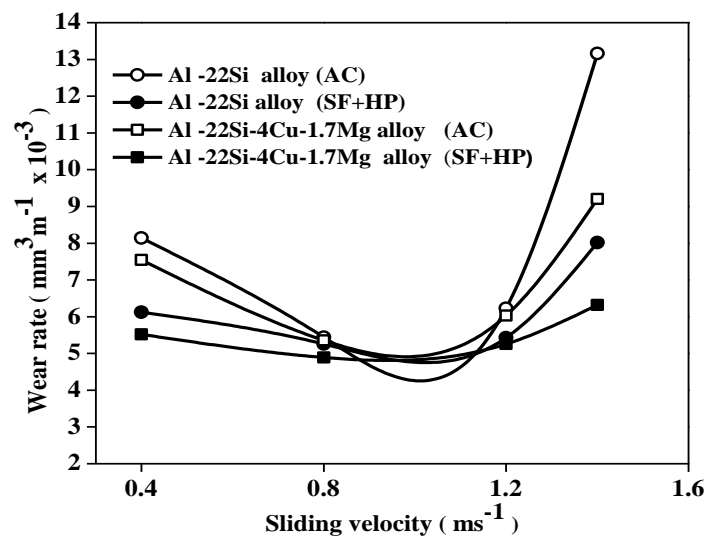
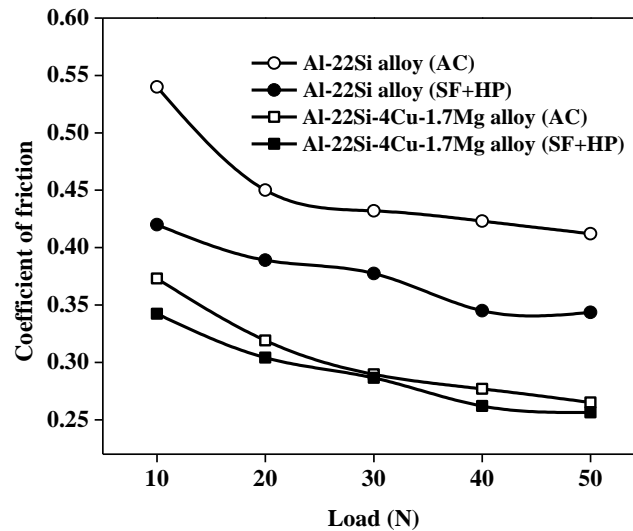


Fig. 8: Variation in wear rate with sliding velocity of AC & SF+HP alloys at a load of 50 N

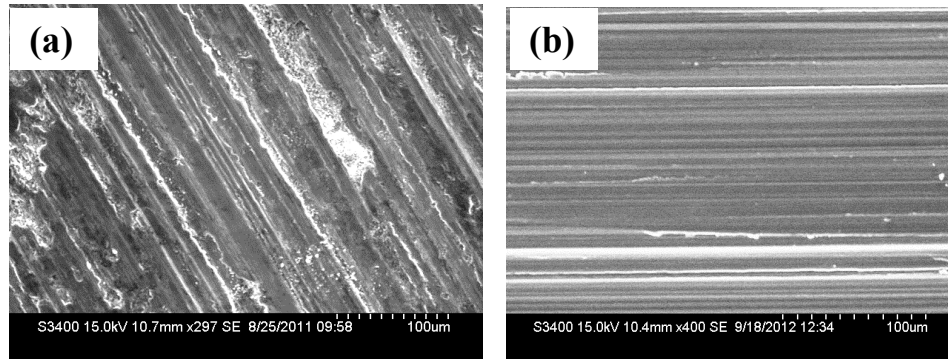


**Fig. 9:** Variation in Coefficient of friction with load of AC and SF + HP alloys

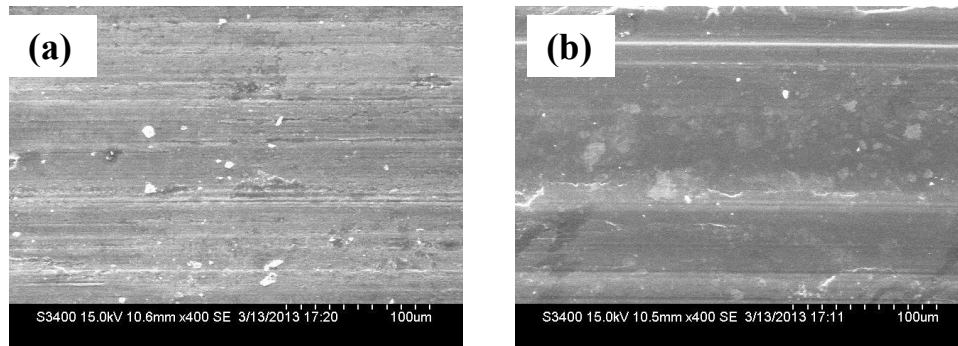
### 3.4 Characterization of worn surfaces

Fig. 10 (a) shows the worn surfaces of as-cast Al-22Si alloy. The surface is characterized by grooves running from one end to the other end of the surface. Large and heavy scoring marks with dimples are present on the surface. The worn tracks and surface damages like micro-grooves, craters and abrasive scoring marks were also clearly observable. Detailed examination of the wear tracks revealed features associated with abrasive and delamination mechanism. The abrasive component of the wear mechanism is pointed out by the plough grooves inside the wear tracks due to the harder silicon particles scratching over the softer (pin) surface. Additionally, the delamination wear component can be concluded from the cracks and shallow craters, which are seen at the worn surface. Some large dimples can also be seen on the worn surface of the alloy, it indicates that block-like primary Si phases were fractured and broken off during wear. Fig. 10 (b) shows the worn surface of SF + HP Al-22Si alloy. The grooves depicted on the worn surface are shallow and uniform. The surface clearly shows a smooth and fine scoring marks and without any pits and dimples that obviously leads to a low wear rate.

The SEM micrographs of worn surfaces of Al-22Si-4Cu-1.7Mg alloys are shown in Fig. 11. The worn surface of as-cast alloy shown in Fig. 11 (a) consists of ploughing marks and a large number of pits indicating a high wear rate. The heavy damage may be due to the presence of long needles of Q-phase and coarse  $\theta$ -Al<sub>2</sub>Cu phase and their uneven distribution in the alloy. It seems that the coarse phases are readily fractured and broken off during wear weakening the matrix leading to a high wear rate. In contrast, the worn surface of spray formed + hot pressed alloy shown in Fig. 11 (b) consists of light scoring marks and shallow dimples in one or two regions clearly indicating a low wear rate. This may be due to the refinement in the microstructure where the Q-phase and  $\theta$ -Al<sub>2</sub>Cu phase have been finely divided and uniformly distributed in the matrix. This fine dispersion provides strength to the matrix and the bonding between these phases and the matrix is strong enough to retain them to the matrix during wear leading to a low wear rate [Wan04].



**Fig. 10:** SEM micrographs of worn out surface of Al-22Si alloys (a) as-cast (b) SF+HP



**Fig. 11:** SEM micrographs of worn surface of Al-22Si-4Cu-1.7Mg alloys (a) as-cast (b) SF+HP

#### 4.0 Conclusions

- I. Spray forming is effective in refining the microstructures of Al-22Si and Al-22Si-5Cu-1.7Mg alloys. The spray deposited Al-22Si alloys exhibited fine and uniform distribution of primary Si and eutectic Si phases and equiaxial morphology of  $\alpha$ -Al phase. The microstructure of spray formed Al-22Si-5Cu-1.7Mg alloy exhibited fine and uniform distribution of both primary and eutectic Si with small needles of Q-intermetallics and  $\theta$ -Al<sub>2</sub>Cu precipitates spread around the boundaries and junctions of grains in  $\alpha$ -Al matrix.
- II. Hot pressing of spray-formed alloys leads to reduction in porosity, grain recovery and recrystallization to certain extent. The spray formed and hot pressed alloys show maximum hardness compared to as-cast alloys.
- III. The spray formed and hot pressed Al-22Si-5Cu-1.7Mg alloy showed maximum hardness compared to other alloys. Wear rate of spray formed Al-22Si-5Cu-1.7Mg alloy is lower than that of Al-22Si alloy under identical sliding conditions. This is because of the presence of fine intermetallics in the former alloy.
- IV. The wear rate of both as-cast and spray formed alloys initially decreases with increase in sliding speed up to a critical speed and then increases but the wear rate is high for as-cast Al-22Si alloy and low for spray formed and hot pressed Al-22Si-5Cu-1.7Mg alloy.

#### References

- [Lai06] Lai S W Lai, Chung D D L: “*Fabrication of particulate aluminum - matrix composites by liquid metal infiltration*”, Journal of Materials Science, 50 (1994), 3128–3150
- [Dhe06] Dheerendra Kumar Dwivedi: “*Wear behavior of cast hypereutectic aluminum silicon alloys*”, Materials and Design, 27 (2006), 610–616

- [Dwi04] Dwivedi D K: “*Sliding temperature and wear behavior of cast Al-Si-Mg alloys*”, Materials Science and Engineering: A , 382 (2004), 328-334
- [Sri06] Srivastava A K, Srivastava V C, Gloter A, Ojha S N: “*Microstructural features induced by spray processing and hot extrusion of an Al-18%Si-5%Fe-1.5% Cu alloy*”, Acta Materialia, 54 (2006), 1741–1748
- [Moh12] Mohamed A M A, Samuel F H: “*A Review on the Heat Treatment of Al-Si-Cu/Mg Casting Alloys, Heat Treatment-Conventional and Novel Applications,*” (2012)
- [Lav96] Lavernia E J, Yu W: “*Spray atomization and deposition*”, John Wiley & Sons Inc. (1996), Chichester (UK)
- [Day13] Dayanand M G, Raju K, Srivastava V C, Rudrakshi G B: “*Effect of secondary processing on the microstructure and wear behavior of spray formed Al-30Mg<sub>2</sub>Si-2Cu alloy*”, Materials and Design 47 (2013), 489–496
- [Sri01] Srivastava V C, Mandal R K, Ojha S N: “*Microstructural Evolution During Spray Forming of Al-18%Si Alloy*”, Journal of Materials Science Letters, 20(2001), 27-29
- [Gra95] Grant P S: *Spray forming*, Progress in Material Science, 39(1995), 497–545
- [Cai98] Cai W D, Lavernia E J: *Modeling of porosity during spray forming: Part-I*”, Metallurgical and Materials Transactions B, 29 (1998), 1085-1096
- [Est90] Estrada J L, Duszczyk J: “*Characteristics of rapidly solidified Al-Si -X preforms produced by the osprey process*”, Journal of Materials Science, 25 (1990), 1381-1391
- [Sha07] Sharma R, Dwivedi D K, “*Solutionizing temperature and abrasive wear behavior of cast Al- Si-Mg alloys*”, Materials and Design, 28 (2007), 975–1981
- [Hau09] Huang L J, Geng L, Li A B, Cui X P, Li H Z, Wang G S: “*Characteristics of hot compression behavior of Ti-6.5Al-3.5Mo-1.5Zr-0.3Si alloy with an equiaxed microstructure*”, Material Science and Engineering A, 505 (2009), 136-143
- [Cla79] Clarke J, Sarkar A D: “*Wear characteristics of as-cast binary aluminum silicon alloys*”, Wear, 54 (1979), 7-16
- [Pra87] Pramila Bai B N, Biswas S K: “*Characterization of dry sliding wear of Al-Si Alloys*”, Wear, 120 (1987), 61-74
- [Sas92] Sasada T, Ban S, Norose S, Nakano T: “*Wear of binary alloys - difference in wear mode between solid solutions and intermetallic compounds*”, Wear, 159 (1992), 191-199
- [Raj12] Raju K, Harsha A P, Ojha S N: “*Effect of microstructure on wear characteristics of spray cast Al-Si alloys*”, Materials Science Forum 710 (2012), 545–550
- [Haq01] Haque M M, Sharif A: “*Study on wear properties of Al-Si piston alloy*”, Journal of Materials Processing Technology 118 (2001), 69–73
- [Ana09] Anasyida A N, Daud A R, Ghazali M J: “*Dry sliding wear behavior of Al-4Si-4Mg alloys by addition of cerium*”, International Journal of Mechanical and Materials Engineering 4 (2009), 12–30
- [Moh96] Mohanty P S, Gruzleski J E: “*Grain refinement mechanisms of hypoeutectic Al-Si alloys*”, Acta Materialia 44 (1996), 360–374
- [Wan04] Wang F, Ma Y, Zhang Z, Cui X, Jin Y: “*A comparison of the sliding wear behavior of a hypereutectic Al-Si alloy prepared by spray-deposition and conventional casting methods*”, Wear 256 (2004), 342–345